ASSESSING VOLTAGE COLLAPSE

R. SEYDEL†

†*Mathematisches Institut, Universität Köln, D-50931 Köln, Germany*
seydel@mi.uni-koeln.de

***Abstract*— Several cases of voltage collapse can be modeled by so-called turning points of the stationary states of special ordinary differential equations. Voltage stability is identified with the margin between the current operating point and the collapse point. Assessing voltage stability then amounts to calculate turning points. This contribution describes different classes of methods to estimate the location of collapse points. One class of approaches is based on test functions, another on curve fitting. The latter approach is the least expensive one.**

***Keywords*— voltage collapse, bifurcation, turning point, computation, risk analysis.**

I. INTRODUCTION

Voltage collapse in power systems has been explained by bifurcation mechanisms. Bifurcation phenomena were observed, for example, when the midwestern segment of the US interconnection system collapsed in 1992 (Kim *et al.*, 1997). For analyzing such events, models of ordinary differential equations (ODEs) have been established. Here we mention the models of the BOARDMAN generator (Nayfeh *et al.*, 1998; Yu, 1983; Zhu *et al.*, 1996), and the model of Dobson and Chiang (1989; Wang *et al.*, 1992). In investigating such models one has found basically two types of bifurcation leading to voltage collapse. The first is the static voltage collapse point, called saddle-node bifurcation or turning point. The second is the dynamic voltage collapse point, mostly Hopf bifurcation.

The essential role bifurcations play for risk has been pointed out earlier (Seydel, 1997b). Broadly speaking, bifurcations are specific states where the quality changes. Most important, stability is lost at bifurcations. The state of a (power) system varies with external parameters such as the power demand. In what follows, this basic parameter of the loading level will be denoted λ. The loading level λ is basically constant but will vary slowly according to the power demand. The desired normal state of operating is to keep λ at an operating point λ_{op} such that the load voltage V remains stable and stationary. If λ exceeds λ_{op} approaching and passing the critical level λ_0 of a bifurcation, the stability of the stationary state is lost, and the dynamical behavior leads to voltage collapse.

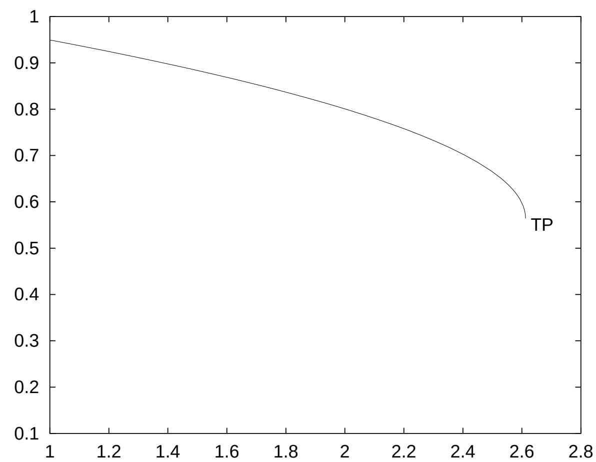

Figure 1: Bifurcation diagram V versus load λ, stationary states of Eq.(2) ($\lambda = Q_1 \geq 1$, upper part of main branch; turning point TP at $\lambda_0 \approx 2.61$).

Figure 1 illustrates a typical saddle-node bifurcation (turning point). The curve represents for each power demand λ in a range $\lambda < 2.6$ the corresponding load level V. For values of λ beyond the critical value $\lambda_0 \approx 2.61$ there is no stable stationary state, which leads to voltage collapse for $\lambda > \lambda_0$. The parabola-like shape of the curve is a manifestation of a saddle-node bifurcation at $\lambda_0 \approx 2.61$. For a situation as depicted in the bifurcation diagram of Fig. 1, the operating point λ_{op} should be significantly smaller than λ_0. The size of the margin between the voltage collapse point λ_0 and the current operating point λ_{op} is used as voltage stability criterion. This margin should be larger than fluctuations d in power demand,

$$\lambda_0 - \lambda_{op} > d + \epsilon. \qquad (1)$$

In Eq.(1) ϵ stands for the absolute error in estimating λ_0. This paper is about calculating approximations to λ_0, the parameter value of a turning point (TP). That is, we shall discuss methods for a static operating point stability assessment. This is primarily a deterministic risk analysis, although measurements, forecasts, and constants may be subjected to probabilistic uncertainties. For an introduction into bifurcation, and for a practical stability analysis, see Seydel (1994).

The reader may also consult *World of Bifurcation* on www.bifurcation.de. For an overview on voltage stability see, for example, Pai and Ajjarapu (1994).

II. EXAMPLE

We shall illustrate methods, results, and phenomena by means of the model of Dobson and Chiang (1989), which we briefly list. The main variables are the reactive power demand $\lambda = Q_1$, the magnitude of the load voltage V, with phase angle δ, the generator voltage phase angle δ_m, and the rotor speed ω. The constants are taken from Wang *et al.* (1992). The model consists of the four ODEs in Eq.(2),

$$\begin{aligned}
\dot{\delta}_m &= \omega \\
M\dot{\omega} &= -d_m\omega + P_m - E_m V Y_m \sin(\delta_m - \delta) \\
K_{q\omega}\dot{\delta} &= -K_{qv2}V^2 - K_{qv}V + Q(\delta_m, \delta, V) \\
&\quad -Q_0 - Q_1 \\
TK_{q\omega}K_{pv}\dot{V} &= K_{p\omega}K_{qv2}V^2 \qquad (2) \\
&\quad +(K_{p\omega}K_{qv} - K_{q\omega}K_{pv})V \\
&\quad +K_{q\omega}(P(\delta_m, \delta, V) - P_0 - P_1) \\
&\quad +K_{q\omega}(P(\delta_m, \delta, V) - P_0 - P_1) \\
&\quad -K_{p\omega}(Q(\delta_m, \delta, V) - Q_0 - Q_1)
\end{aligned}$$

with variables

$P(\delta_m, \delta, V) = -E_0 V Y_0 \sin(\delta) + E_m V Y_m \sin(\delta_m - \delta)$
$Q(\delta_m, \delta, V) = E_0 V Y_0 \cos(\delta) + E_m V Y_m \cos(\delta_m - \delta) - (Y_0 + Y_m)V^2$

and constants

$M = 0.01464,\ Q_0 = 0.3,\ E_0 = 1.0,\ E_m = 1.05,\ Y_0 = 3.33,\ Y_m = 5.0,\ K_{p\omega} = 0.4,\ K_{pv} = 0.3,\ K_{q\omega} = -0.03,\ K_{qv} = -2.8,\ K_{qv2} = 2.1,\ T = 8.5,\ P_0 = 0.6,\ P_1 = 0.0,\ C = 12.0,\ P_m = 1.0,\ d_m = 0.05.$

Figures 1 and 2 summarize basic solution behavior of this model. The lower half of the parabola-like curve (skipped in Fig. 1) consists entirely of unstable states; they are not reached in a real experiment but leave a trace, and they can be easily calculated. Figure 2 depicts both stable and unstable solutions of Eq.(2). The solid curve in Fig. 2 consists of stationary states. The shape illustrates the name turning point for the saddle-node bifurcation at the right end. The dashed curves represent periodic orbits; they will be discussed in the final part of this paper.

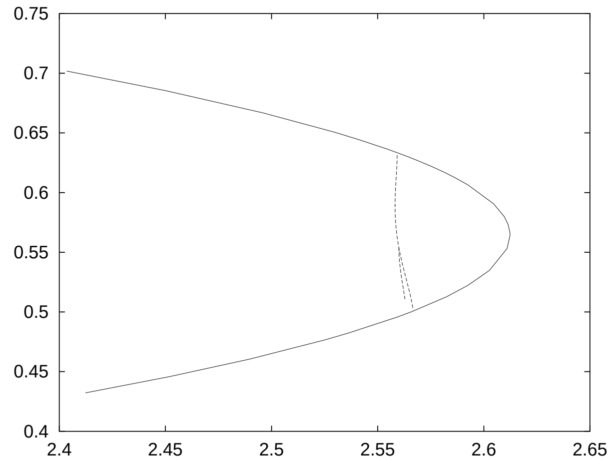

Figure 2: Bifurcation diagram V versus load λ (detail: $\lambda \geq 2.41$, all stationary states, and dashed the $V_{\min}$ of some periodic states).

III. BASIC PRINCIPLES OF NUMERICAL BIFURCATION

This section summarizes some fundamental approaches of numerical bifurcation. Let the ODE that models a power system be written as

$$\dot{\mathbf{y}} = \mathbf{f}(\mathbf{y}, \lambda), \qquad (3)$$

where $\mathbf{y}(t)$ is a vector function with n components $y_i(t)$, $i = 1, \ldots, n$. For Eq.(2), $n = 4$. The overdot indicates differentiation with respect to time t, and $\mathbf{f}$ is the right-hand side defining the dynamical law. The state $\mathbf{y}$ that solves Eq.(3) depends on the real parameter λ. Stationary solutions $\mathbf{y}^s$ of (3) solve

$$\mathbf{f}(\mathbf{y}^s, \lambda) = \mathbf{0}. \qquad (4)$$

Periodic solutions of the autonomous system of Eq.(3) satisfy $\mathbf{y}(t + T) = \mathbf{y}(t)$ for all t and a minimum period $T > 0$. A continuum of solutions $(\mathbf{y}, \lambda)$ is called a *branch.* The curves in Fig. 2 represent branches. Branches are traced by continuation methods. The first task during branch tracing is to detect bifurcations, which are denoted $(\mathbf{y}_0, \lambda_0)$.

Bifurcation test functions provide a framework for procedures designed to detect bifurcations. Such a test function $\tau(\mathbf{y}, \lambda)$ is evaluated along a branch during continuation. The basic feature of a test function for detecting a bifurcation $(\mathbf{y}_0, \lambda_0)$ is $\tau(\mathbf{y}_0, \lambda_0) = 0$. That is to say, the bifurcation is a zero of the test function. Moreover, we require τ to be continuous in a neighborhood of the bifurcation, and to change sign at $(\mathbf{y}_0, \lambda_0)$. With such a test function at hand, the remaining exercise is to detect zeros of τ during branch tracing. In the context of voltage collapse, test functions have also been called *index.*

An important example of test functions is provided by the eigenvalues of the Jacobian matrix $\mathbf{f_y}(\mathbf{y}, \lambda)$. In case the eigenvalues $\mu_1, \ldots, \mu_n$ of the Jacobian matrices are calculated, the test function

$$\tau := \max\{\mathrm{Re}(\mu_1), \ldots, \mathrm{Re}(\mu_n)\} \qquad (5)$$

indicates stability by its sign. This test function detects those bifurcations that separate stable from unstable stationary solutions. Another test function will be defined below in Eq.(9).

Bifurcation points (such as turning points) can be calculated with high accuracy. The idea of calculating a bifurcation of $\mathbf{f}(\mathbf{y},\lambda) = \mathbf{0}$ is to set up an equation $\mathbf{F}(\mathbf{y},\lambda) = \mathbf{0}$ which selectively and exclusively has a bifurcation $(\mathbf{y}_0,\lambda_0)$ as solution. Then each solution procedure applied to $\mathbf{F}(\mathbf{y},\lambda) = \mathbf{0}$ provides an iteration to calculate $(\mathbf{y}_0,\lambda_0)$. Basically, the equation consists of

$$\mathbf{F}(\mathbf{y},\lambda) := \begin{pmatrix} \mathbf{f}(\mathbf{y},\lambda) \\ \tau(\mathbf{y},\lambda) \end{pmatrix} = \mathbf{0} \qquad (6)$$

with τ being a bifurcation test function.

A successful realization of Eq.(6) has attached the linearization, and characterizes $(\mathbf{y}_0,\lambda_0)$ by a Jacobian $\mathbf{f_y}$ having a zero eigenvalue with right eigenvector $\mathbf{h}_0$. The resulting *branching system* of Seydel (1979)

$$\mathbf{F}(\mathbf{y},\lambda,\mathbf{h}) := \begin{pmatrix} \mathbf{f}(\mathbf{y},\lambda) \\ \mathbf{f_y}(\mathbf{y},\lambda)\mathbf{h} \\ h_k - 1 \end{pmatrix} = \mathbf{0} \qquad (7)$$

has the dimension $2n+1$.

The solution of the branching system includes $\mathbf{y}_0$, λ_0, and the right eigenvector $\mathbf{h}_0$. This vector $\mathbf{h}_0$ can be embedded into a continuous family of vectors $\mathbf{h}$ defined also for solutions $(\mathbf{y},\lambda)$ different from $(\mathbf{y}_0,\lambda_0)$. This function $\mathbf{h} = \mathbf{h}(\mathbf{y},\lambda)$, which satisfies $\mathbf{h}(\mathbf{y}_0,\lambda_0) = \mathbf{h}_0$, is defined by the equation

$$[(\mathbf{I} - \mathbf{e}_l\mathbf{e}_l^{tr})\mathbf{f_y}(\mathbf{y},\lambda) + \mathbf{e}_l\mathbf{e}_k^{tr}]\mathbf{h} = \mathbf{e}_l. \qquad (8)$$

(^{tr} means transposure.) The vectors $\mathbf{e}_l$, $\mathbf{e}_k$ are canonical unit vectors for suitably chosen indices l, k. The defect of $\mathbf{f_y}(\mathbf{y},\lambda)\mathbf{h}$ indicates the distance to the bifurcation, and gives rise to a test function,

$$\tau = \tau_{lk}(\mathbf{y},\lambda) := \mathbf{e}_l^{tr}\mathbf{f_y}(\mathbf{y},\lambda)\mathbf{h}. \qquad (9a)$$

Since $\mathbf{f_y}(\mathbf{y},\lambda)^{tr}\mathbf{e}_l = \text{grad } f_l(\mathbf{y},\lambda) =: \nabla f_l(\mathbf{y},\lambda)$, an equivalent way of writing (9a) is

$$\tau_{lk} = \nabla f_l^{tr}\mathbf{h}. \qquad (9b)$$

Geometrical implications and the interpretation of a suitably scaled τ as angle are straightforward. The test functions of Eq.(9) qualify to detect singularities of the Jacobian provided that the indices l, $k \in \{1,...,n\}$ satisfy the criterion

$$h_k \neq 0, \quad g_l \neq 0, \qquad (10)$$

where g_l is the l-th component of the left eigenvector $\mathbf{g}$ of $\mathbf{f_y}(\mathbf{y}_0,\lambda_0)$ (Seydel, 1979, 1991, 1997a).

IV. COMPUTATION OF TURNING POINTS / STATIC VOLTAGE COLLAPSE POINTS

The above principles lend over to algorithms for the computation of turning points. The algorithms will be illustrated with results obtained for the example of Eq.(2). We discuss three classes of methods, focussing on one representative of each. We distinguish among the class of direct methods, the class of methods based on the geometry of the branches, and the class of methods exploiting test functions.

A. Direct methods.

The most accurate method is to set up the branching system of Eq.(7), and to solve it. The solution can be performed either by calling standard software of numerical analysis, or by exploiting the block structure of Eq.(7). In both cases, a good initial guess must be provided, which can be obtained during continuation (Seydel, 1994). Since for Eq.(2) the dimension $n = 4$ is small, the solution of Eq.(7) is straightforward. We choose Newton's method, and obtain the values of the turning point

$$\lambda_0 = 2.6123712847, \quad V_0 = 0.5642346744. \qquad (11)$$

Mostly, the accuracy delivered by solving the branching system exceeds by far the accuracy of the modelling. Hence, in practice, it often takes too much effort to solve Eq.(7). This holds in particular for larger values of the dimension n, which are characteristic for the voltage collapse problems reported in Souza *et al.* (1997). Here we shall use the results of Eq.(11) for reference only in order to calculate the errors of the results obtained by other methods. Methods that solve just one suitably constructed equation are called *direct methods.*

B. Methods based on the geometry of the branch.

The cheapest methods exploit the geometrical shape of the branches (see Figures 1 and 2). Locally, in a neighborhood of the turning point, the branch behaves like a parabola. This holds for each of the (y_i,λ)-planes, hence one has n parabolas. Since a parabola is defined by three points, we require three solutions along the branch in order to construct an interpolating parabola. To set up a formula, we concentrate on the (V,λ)-plane, $y_4 = V$, and denote the relevant data of three calculated solutions of Eq.(4)

$$(V_1,\lambda_1),\ (V_2,\lambda_2),\ (V_3,\lambda_3).$$

The interpolating parabola $\lambda = P(V)$ itself may be without interest, but the value (V,λ) for which

$$\frac{d\lambda}{dV} = \frac{dP}{dV} = 0 \qquad (12)$$

holds is an approximation $(\bar{V}_0,\bar{\lambda}_0)$ of the turning point (V_0,λ_0). The result of the simple calculus related to Eq.(12) (Exercise 5.9 in Seydel, 1994) is

$$\begin{aligned} \zeta_1 &:= (\lambda_2 - \lambda_1)/(V_2 - V_1), \\ \zeta_2 &:= (\lambda_3 - \lambda_1)/(V_3 - V_1), \\ \gamma &:= (\zeta_2 - \zeta_1)/(V_3 - V_2), \\ \bar{V}_0 &:= \tfrac{1}{2}(V_1 + V_2 - \zeta_1/\gamma) \\ \bar{\lambda}_0 &:= \lambda_1 + (\bar{V}_0 - V_1)\cdot[\zeta_1 + \gamma(\bar{V}_0 - V_2)]. \end{aligned} \qquad (13)$$

Evaluating this formula costs almost nothing compared to the costs in solving Eq.(4). Since during continuation a series of solution points (V_j,λ_j) are calculated, a choice must be made of which three points are selected. The closer the points are situated near λ_0 the better are the results. This is illustrated in Table 1. The error also depends in an unknown way on the choice of the component. For example, if the approximation (13) would have been based on δ_m rather than on V, the relative errors (last row in Table 1) would have been $0.089/0.00013/0.35 * 10^{-5}$.

λ_1	1.32772	2.30846	2.60964
λ_2	1.82133	2.56455	2.61149
λ_3	2.30846	2.61149	2.61233
$\bar{V}_0$	0.55957	0.56364	0.56422
$\bar{\lambda}_0$	2.61940	2.61247	2.61237
rel. error	0.00269	0.00004	$0.14 * 10^{-6}$

Table 1: Three approximations $(\bar{V}_0, \bar{\lambda}_0)$ of the turning point (V_0, λ_0). The relative error shown is $|\lambda_0 - \bar{\lambda}_0|/|\lambda_0|$ for λ_0 from (11). The entries are rounded in the last decimal digit.

The interpolation of the branch by means of a parabola can be replaced by other curve-fitting approaches. The quality of the approximation depends on the smoothness of the branch. For example, one may use polynomials $\lambda = P(V)$ of higher order, again exploiting Eq.(12). This amounts to inverse interpolation to the zero of $\frac{dP}{dV}$. We do not present details because we do not expect significantly better results. Least squares approximations are possible too, but are not included in this test.

C. Methods based on test functions.

The derivative $d\lambda/dV$ exploited in Eq.(12) can be seen as a test function for turning points, $\tau = \left(\frac{dV}{d\lambda}\right)^{-1}$. But this index is again based on the geometry, see the previous subsection. In this subsection we discuss test functions that are more involved, and that introduce further information. Typically such *test functions measure the singularity* of the Jacobian matrices in some way. Examples have been furnished in Eq.(5) and in Eq.(9). Another possibility is to calculate the singular values of the matrices. To apply a test function we assume that its values τ have been calculated in addition to the solutions $(\mathbf{y}, \lambda)$. That is, we assume that several triples $(\mathbf{y}, \lambda, \tau)$ have been calculated along the branch. Note that providing τ can be quite expensive. (For the test function (9) an inexpensive evaluation has been proposed in Seydel (1991.)

In order to calculate a zero of the chosen test function τ, standard methods of interpolation can be applied. Since this is done analogously as in the previous subsection, we omit related tests. Instead we concentrate on the attractive possibility to calculate an approximation $\bar{\lambda}_0$ based on the data of just *one* solution. To this end we use the test function of Eq.(9), calculate the derivative $d\tau/d\lambda$ (Seydel, 1979), and use the estimate

$$\bar{\lambda}_0 = \lambda - \frac{\tau(\lambda)}{2\tau'(\lambda)}, \qquad (14)$$

which exploits a parabolic shape of τ close to turning points. Equation (14) corresponds to the fact that an interpolating parabola $\lambda = P(\tau)$ is defined by two points. Since $n = 4$ in Eq.(2) there are at most $16 = 4^2$ test functions in Eq.(9). Some of them violate the local criterion (10). Monitoring all test functions it turns out that 12 of the test functions survive. Thus the chances to pick a valid (l, k)-combination are high when we just choose index pairs at random. (It is not realistic to really check the local criterion (10) when we are far from $(\mathbf{y}_0, \lambda_0)$.) Instead of a random choice of l, k we may exploit the *sensitivity result* of Seydel (1991):

> The test function of Eq.(9) monitors how the component f_l varies when the solution $\mathbf{y}$ is varied in the direction determined by $\mathbf{h}$.

Hence, from the physical background of the functions f_l of the right-hand side of Eq.(3) one may deduce which choice of l, k is not promising. (For the example of Eq.(2), $k = 2$ is not suitable.) We note in passing that the largest absolute component of the vector $\mathbf{h}$ of Eq.(8) can be used to identify critical buses (Souza *et al.*, 1997). We show some results for the choice $l = 3$, $k = 1$; results based on the other possible choices are analogous.

λ	τ	$\bar{\lambda}_0$
2.0956	−6.2437	3.6064
2.4620	−5.1431	2.9702
2.5805	−4.0568	2.6605
2.6019	−3.2986	2.6255
2.6079	−2.7012	2.6166
2.6114	−1.7472	2.6130
2.6124	+0.1529	2.6124

Table 2: Single-solution based approximation $\bar{\lambda}_0$, using Eq.(14).

Comparing the quality of the approximations of Table 2 with those of Table 1, it becomes evident that calculating $\bar{\lambda}_0$ based on the data of just one solution is not competitive. The assumption was made because of the high costs of evaluating test functions that monitor the singularity. Of course, evaluating τ and τ' is not cheaper than evaluating τ at two solutions.

V. CONCLUSIONS

We have discussed three classes of methods for calculating the turning points relevant to voltage collapse. All of the above methods have been suggested earlier by this author. Several of the ideas have been applied and discussed in recent publications, see for instance Ejebe *et al.* (1996), Pai and Ajjarapu (1994), Souza *et al.* (1997), and Wang and Girgis (1996).

Direct methods are highly recommendable in the rare cases where extreme accuracy is required. In addition, direct methods are most comfortable in cases when a second parameter is varied for a *sensitivity analysis*, which is an important task for assessing voltage stability (Greene *et al.*, 1997; Seydel, 1997b).

If only one parameter is varied at a time (our λ), then continuation-based curve-fitting approaches provide good accuracy most efficiently. This holds for those approaches that exploit the geometry of the branches, which is delivered as byproduct of continuation. Evaluating singularity-based test functions is more expensive. This holds in particular if they are needed for all of the calculated solutions $(\mathbf{y}, \lambda)$ of Eq.(4). In summary, the simple parabola method of Section IV.B is most recommendable to estimate the location of the turning points, and to provide information on risk assessment using Eq.(1). Another advantage of the geometry-based approach is that it can be based on experiments if no trustworthy model ODE is known.

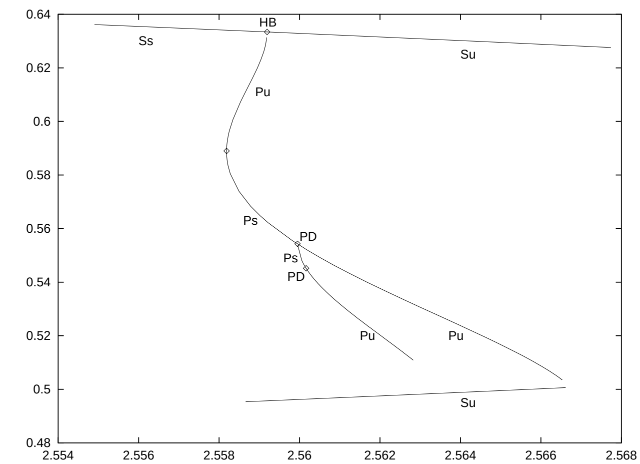

Figure 3: Same as Fig. 2, but detail $2.555 \leq \lambda \leq 2.568$. (S: stationary, P: periodic, s: stable, u: unstable, HB: Hopf bifurcation, PD: periodic doubling)

VI. OUTLOOK

As is well-known there are voltage collapse phenomena not caused by turning points. For example, Hopf bifurcation plays an important role initiating voltage collapse (Abed and Varaiya, 1984; Abed *et al.*, 1993; Nayfeh *et al.*, 1998; Ohta and Ueda, 1998; Pai and Ajjarapu, 1994; Zhu *et al.*, 1996). Also for the example of Eq.(2) Hopf bifurcation is decisive: The stability of the stationary branch is "already" lost at $\lambda_{\text{HOPF}} = 2.55919$, and stable periodic orbits, period doublings (flip bifurcations, the first at $\lambda_{\text{PD}} = 2.55996$), blue-sky bifurcation, and chaos occur shortly "before" the turning point (Abed *et al.*, 1993; Wang *et al.*, 1992). Several of these dynamic phenomena preceding the turning point are indicated in Fig. 3. Figure 4 illustrates the mechanism of a metamorphosis towards a blue-sky bifurcation caused by the "lower" unstable stationary state (Su in Fig. 4). This emphasizes the fundamental role unstable states play in organizing dynamic behavior. (The results reported by the figures have been calculated by means of BIFPACK, see Seydel, 1994.)

For assessing Hopf bifurcations the geometry of the stationary branch does not help (see the top curve in Fig. 3). Here the methods of the class in Section IV.B are not relevant, and typically eigenvalue-based test functions are used. For large systems (n large) there are special methods, see Kim *et al.* (1997), and Neubert (1993). Such risk studies stress the importance to be able to calculate bifurcations, and to calculate unstable states.

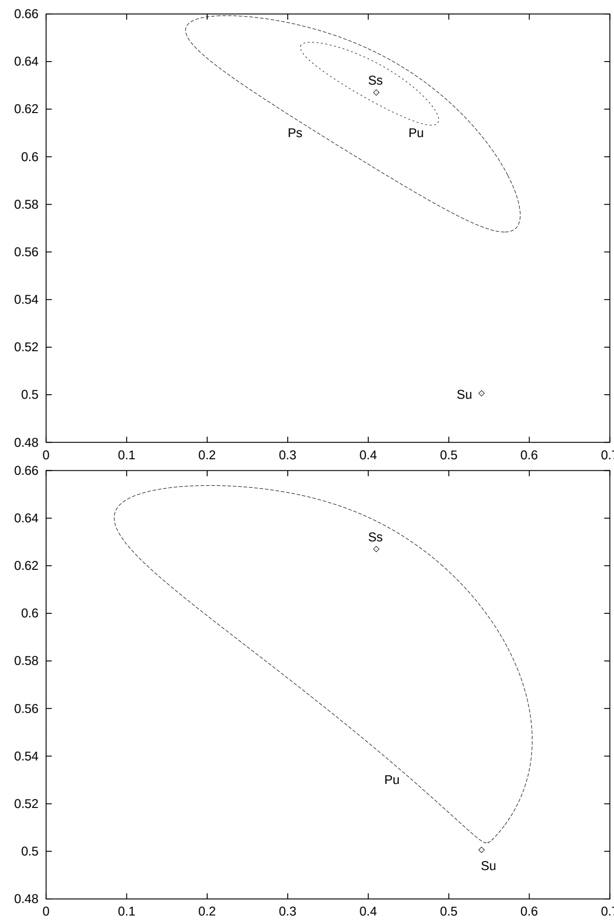

Figure 4: Phase diagrams (projection). Horizontal axis: δ_m; vertical axis: V. top: $\lambda = 2.5588$, bottom: $\lambda = 2.5665$

REFERENCES

Abed, E. H. and P. P. Varaiya, "Nonlinear Oscillations in Power Systems," *Int. Journal on Electric Power and Energy Systems* **6**, 37–43 (1984).

Abed, E. H., H. O. Wang, J. C. Alexander, A. M. A. Hamdan and H.-C. Lee, "Dynamic Bifurcations in a Power System Model Exhibiting Voltage Collapse," *Int. J. of Bifurcation and Chaos* **3**, 1169–1176 (1993).

Dobson, I. and H.-D. Chiang, "Towards a Theory of Voltage Collapse in Electric Power Systems," *Systems and Control Letters* **13**, 253–262 (1989).

Ejebe, G. C., G. D. Irisarri, S. Mokhtari, O. Obadina, P. Ristanovic and J. Tong, "Methods for Contingency Screening and Ranking for Voltage Stability Analysis of Power Systems," *IEEE Transactions on Power Systems* **11**, 350–356 (1996).

Greene, S., I. Dobson and F. L. Alvarado, "Sensitivity of the Loading Margin to Voltage Collapse with Respect to Arbitary Parameters," *IEEE Transactions on Power Systems* **12**, 262–268 (1997).

Kim, K., H. Schättler, V. Venkatasubramanian, J. Zaborsky and P. Hirsch, "Methods for Calculating Oscillations in Large Power Systems," *IEEE Transactions on Power Systems* **12**, 1639–1648 (1997).

Nayfeh, A. H., A. M. Harb, C.-M. Chin, A. M. A. Hamdan and L. Mili, "Application of Bifurcation Theory to Subsynchronous Resonance in Power Systems," *Int. J. of Bifurcation and Chaos* **8**, 157–172 (1998).

Neubert, R., "Predictor-Corrector Techniques for Detecting Hopf Bifurcation Points," *Int. J. of Bifurcation and Chaos* **3**, 1311–1318 (1993).

Ohta, H. and Y. Ueda, "Global Bifurcation Caused by Unstable Limit Cycle Leading to Voltage Collapse in an Electric Power System," *Chaos, Solitons and Fractals* **9**, 825–843 (1998).

Pai, M. A. and V. Ajjarapu, "Voltage Stability in Power Systems – An Overview," In: *Recent Advances in Control Management of Energy Systems* (Ed.: D. P. Sengupta et al.) Interline Publishing, Bangalore, 189–218 (1994).

Seydel, R., "Numerical Computation of Branch Points in Nonlinear Equations," *Numer. Math.* **33**, 339–352 (1979).

Seydel, R., "On Detecting Stationary Bifurcations," *Int. J. of Bifurcation and Chaos* **1**, 335–337 (1991).

Seydel, R., *Practical Bifurcation and Stability Analysis*, Second Edition, Springer Interdisciplinary Applied Mathematics, Volume 5, New York (1994).

Seydel, R., "On a Class of Bifurcation Test Functions," *Chaos, Solitons and Fractals* **8**, 851–855 (1997a).

Seydel, R., "Risk and Bifurcation: Towards a Deterministic Risk Analysis," In: *Risk Analysis and Management in a Global Economy. Risk Management in Europe: New Challenges for the Industrial World*, Center of Technology Assessment, Stuttgart, 318–339 (1997b).

Souza, A. C. Z. de, C. A. Cañizares and V. H. Quintana, "New Techniques to Speed Up Voltage Collapse Computations Using Tangent Vectors," *IEEE Transactions on Power Systems* **12**, 1380–1387 (1997).

Wang, H., E. H. Abed and A. M. A. Hamdan, "Is Voltage Collapse Triggered by the Boundary Crisis of a Strange Attractor?" *Proc. American Control Conference*, Chicago (1992).

Wang, L. and A. A. Girgis, "Online Detection of Power Systems Small Disturbance Voltage Instability," *IEEE Transactions on Power Systems* **11**, 1312–1313 (1996).

Yu, Y., *Electric Power System Dynamics*, Academic Press, New York (1983).

Zhu, W., R. R. Mohler, R. Spee, W. A. Mittelstadt and D. Maratukulam, "Hopf Bifurcations in a SMIB Power System with SSR," *IEEE Transactions on Power Systems* **11**, 1579–1584 (1996).

in *Latin American Applied Research*, special issue on **Bifurcation Control: Methodologies and Applications 31**,3 (2001) 171-176.